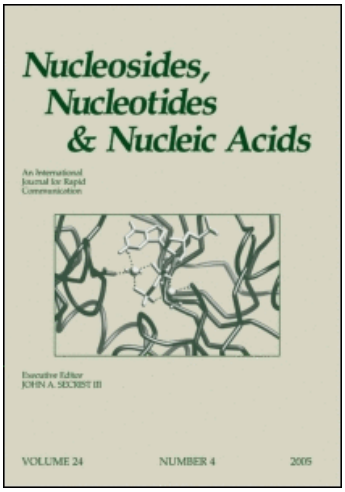

Nucleosides, Nucleotides and Nucleic Acids
Publication details, including instructions for authors and subscription information:
http://www.informaworld.com/smpp/title~content=t713597286

Electrochemical Study on Behavior of $EuMo_2$ Complex and Its Interaction With DNA

Zhifeng Li[a]; Jingwan Kang[b]; Xiaoquan Lu[b]
[a] School of life Science and Chemistry, Tianshui Normal University, Tianshui, P.R. China [b] Department of Chemistry, Northwest Normal University, Lanzhou, P.R. China

To cite this Article Li, Zhifeng , Kang, Jingwan and Lu, Xiaoquan(2007) 'Electrochemical Study on Behavior of $EuMo_2$ Complex and Its Interaction With DNA', Nucleosides, Nucleotides and Nucleic Acids, 26: 1, 9 — 22
To link to this Article: DOI: 10.1080/15257770601052232
URL: http://dx.doi.org/10.1080/15257770601052232

Nucleosides, Nucleotides, and Nucleic Acids, 26:9–22, 2007

ISSN: 1525-7770 print / 1532-2335 online
DOI: 10.1080/15257770601052232

Taylor & Francis
Taylor & Francis Group

ELECTROCHEMICAL STUDY ON BEHAVIOR OF $EuMo_2$ COMPLEX AND ITS INTERACTION WITH DNA

Zhifeng Li □ *School of life Science and Chemistry, Tianshui Normal University, Tianshui, P.R. China*

Jingwan Kang and Xiaoquan Lu □ *Department of Chemistry, Northwest Normal University, Lanzhou, P.R. China*

□ *The electrochemical behavior of complex $EuMo_2$ (Mo = Morin, 2′,3,4′5,7-pentahydroxyflavone) and its interactions with calf thymus DNA were studied using cyclic voltammetry (CV) and double potential step chronocoulometry (DPSCC) at glass carbon electrode (GCE) and DNA modified GCE, respectively. Information such as diffusion coefficient (*D*), rate constant (k_s) of $EuMo_2$ and intrinsic binding constant (*K*), binding numbers (n) of bound species per DNA (bp) were obtained. $EuMo_2$ can bind to DNA, and the binding mode is intercalation. By nonlinear fitting with Langmuir equation, a K of 1.02 × 10^6 M^{-1} and an n of 1 were obtained.*

Keyword $EuMo_2$ complex; Calf thymus DNA; Intercalation mode; DNA modified electrode

1. INTRODUCTION

Nucleic acids offer the analytical chemist a powerful tool in the recognition and monitoring of many important compounds. The interaction of DNA with other molecules is an important fundamental issue in life sciences. Investigations based on DNA interactions with small molecular compounds have great importance in understanding the mechanisms of action of some antitumor and antiviral drugs and origins of some diseases and to design new DNA-targeted drugs and also to screen these drugs in vitro. The interactions of some anticancer drugs with DNA have been studied by a variety of techniques.[1–5] In recent years, there is a growing interest in the electrochemical investigations of interactions between anticancer drugs

Received 4 November 2005; accepted 15 June 2006.
The present work was supported by a grant from the National Natural Science foundation of China (No. 20275031, 20335030) and KJCXGC-01 from Northwest Normal University.
Address correspondence to J. W. Kang, Department of Chemistry, Northwest Normal University, Lanzhou 730070, P.R. China. E-mail: jwkang@nwnu.edu.cn

and other DNA targeted molecules and DNA.[6–8] Recently, a modified layer of DNA biopolymer immobilized on the electrode surface has been successfully used for the accumulation of trace analytes including drugs and potential pollutants, the recognition of specific base sequences of DNA and the elucidation of the mechanism of drugs action.[9–18] DNA-modified electrodes have been suggested a sensor for the detection of damage to double stranded DNA (dsDNA). DNA biosensor technologies are currently under intense investigation owing to their great promise for rapid and low-cost detection of specific DNA sequences in human, viral and bacterial nucleic acid.[19]

Flavonoids are nonnutritive compounds of plants that recently have aroused considerable interest due to their broad pharmacological activity, such as antiviral, antiallergic, antiplatelet, anti-inflammatory, antitumor activities, and possibly even protective effects against chronic diseases.[20–22] However, the literature on the electrochemical investigation of flavonoids is limited.[23–26] Morin is an important kind of flavonoid. Flavonoids complexate with metal cations to form stable complexes, which have demonstrated antibacterial properties and antitumor activities and have been used in the spectral analysis of metal ions.[4,5,8,19,30,31] Rare earth elements have been found to be physiologically active, and also to have decreased toxicity after coordinating with a ligand.[27] A study of the interaction between $EuMo_2$ complexes and DNA is important to further understand the pharmacology of Morin and Europium. In this paper, the electrochemical methods of CV and DPSCC, spectral methods of UV-vis and fluorescence are employed. Some electrochemical information was also obtained using surface electrochemical methods.

2. EXPERIMENTAL

2.1. Reagents

Morin was obtained from Chemical Reagent Co. of the Chinese Academy of Sciences, (Lanzhou, China). It was dissolved in ethanol and doubly distilled water to give stock solution. Eu_2O_3 was purchased from The Gansu Rare Earth Co. (Gansu, China). The stock solution of Eu^{3+} was prepared by dissolving Eu_2O_3 in a minimum amount of perchloric acid and diluting with doubly distilled water. Calf thymus DNA was purchased from The Sino-American Biotechnology Co. (Beijing China) and used as received. Native double-stranded DNA (dsDNA) was dissolved in doubly distilled water. Its stock solutions were stored at 4°C. Ratios of UV absorbance of DNA at 260 and 280 nm, A_{260}/A_{280}, of 1.8–1.9, indicate that the DNA was sufficiently free of protein. Other reagents were of analytical grade. Experiments were conducted in 0.1 M HOAc–NaOAc buffer solution at pH 6.4 containing 50 mM KCl.

2.2. Instrumentation

CHI-832 electrochemical Analyzer (CH Instruments, Ltd. Co., Austin, TX, USA) with a three-electrode system, including working electrode (bare glass carbon, a dsDNA modified glass carbon or a platinum disk), a counter electrode of platinum wire and a saturated calomel reference electrode (SCE). The bare glass carbon electrode area is 1.37×10^{-2} cm^2. Branson 200 Ultrasonic cleaner UV-vis spectra were obtained with an Agilent–8453 Spectrophotometer (USA). RF–540 spectrofluorophometer (Hitachi, Japan). Experiments were carried out at the laboratory temperature (25°C).

2.3. Preparation of dsDNA-Modified Glass Carbon Electrode (dsDNA–GCE)

The preparation methods for dsDNA-GCE followed the literature.[28] A glass carbon electrode was first polished successively with 0.1 and 0.05 μm alpha alumina powder and then cleaned ultrasonically in water and acetone respectively for 5 minutes. The freshly-pretreated glass carbon electrode was modified by transferring a drop of 1 mg mL^{-1} dsDNA solution onto its surface, followed by air-drying overnight. Then, it was soaked in double distilled water for more than 4 hours to remove unabsorbed dsDNA and a dsDNA–GCE was obtained.

2.4. Procedure

In 0.1 M HOAc–NaOAc (pH 6.4) buffer solution containing Eu^{3+} and Morin was added to the volume cell, deoxygenated with nitrogen for 5 minutes then the CV and DPSCC detections were carried out. The formation of the $EuMo_2$ complex was conducted by keeping concentration of Eu^{3+} constant and varying concentration of Morin using a platinum disk as the working electrode, and other experiments were carried out using a bare GCE or a dsDNA-modified GCE as the working electrode.

DPSCC measurements were performed after a dsDNA–GCE was soaked in test solution for 2–3 minutes to ensured equilibration between DNA on the electrode surface and test species in solution.

The UV-visible titration of Morin with Eu^{3+} was conducted by keeping the concentration of Morin constant and varying Eu^{3+} concentration.

3. RESULTS AND DISCUSSION

3.1. Interaction of Morin with Eu^{3+}

The cyclic voltammogram of 3.0×10^{-4} M Eu^{3+} has a pair of quasi-reversible redox peaks at -0.481 V (E_{pc}) and -0.393 V (E_{pa}), respectively, with ΔE (E_{pa}-E_{pc}) = 90 mV in the 0.1 M HOAc–NaOAc (pH 6.4) buffer solution for bare glass carbon electrode (Figure 1a). After addition of

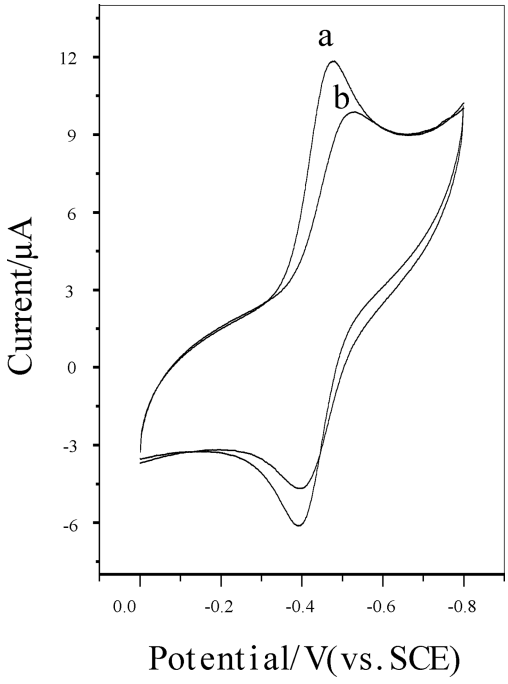

FIGURE 1 Cyclic voltammograms of 1.0×10^{-4} M Eu^{3+} (a) and 1.0×10^{-4} M Eu^{3+} + 2.0×10^{-4} M Morin (b) in 0.1 M HOAc–NaOAc, pH 6.0, buffer containing 50 mM KCl at bare glass carbon electrode; scan rate, 80 mVs^{-1}.

1.0×10^{-4} M Morin to 3.0×10^{-4} Eu^{3+}, the redox peak currents decrease markedly and E_{pc} and E_{pa} shift to more negative values to −0.531 V and −0.398 V (Figure 1b). ΔE (E_{pa}-E_{pc}) = 133 mV shows that the process became irreversible. These electrochemical behaviors show that there is strong interaction between Eu^{3+} and Morin and they can form a $EuMo_n$ complex on the glassy carbon electrode.

According to the literature,[29] it is assumed that the interaction of Morin with Eu^{3+} only produces a single complex $EuMo_n$:

$$Eu^{3+} + nMo \rightleftharpoons Eu - Mo_n \tag{1}$$

The equilibrium constant is as follows:
And the following equations can be deduced:

$$K' = \frac{[Eu - Mo_n]}{[Eu^{3+}][Mo]^n} \tag{2}$$

$$\Delta I_{max} = KC_{Eu^{3+}} \tag{3}$$

$$\Delta I = K[Eu - Mo] \tag{4}$$

$$[Eu^{3+}] + [Eu - Mo_n] = C_{Eu^{3+}} \tag{5}$$

$$\Delta I_{Max} - \Delta I = K[Eu^{3+}] \tag{6}$$

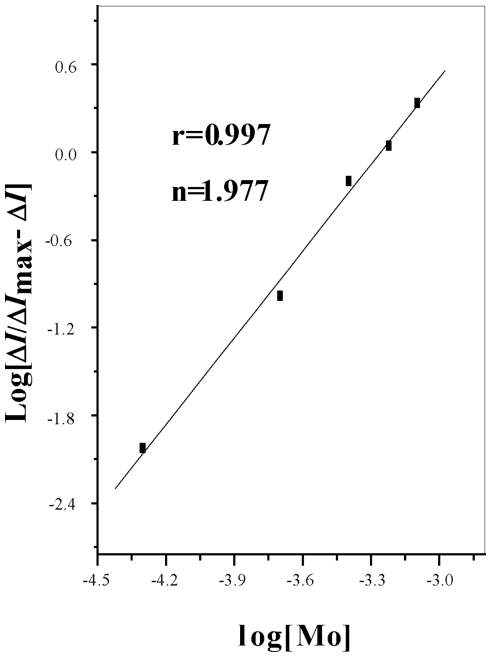

FIGURE 2 Relationship between $\lg[\Delta I/(\Delta I_{max}\text{-}\Delta I)]$ and lg[Mo], Eu^{3+}, 1.0×10^{-4} M.

Introducing Equations (4) and (6) into Equation (2), leads to

$$\lg \frac{\Delta I}{\Delta I_{\max} - \Delta I} = \lg K' + n \lg[Mo] \tag{7}$$

If interaction of Eu^{3+} with Morin forms a single complex, according to the Equation (7), the plot of $\lg\Delta I/(\Delta I_{max}\text{-}\Delta I)$ vs. lg[*Mo*] would show a linear line with a slope of n. Figure 2 indicates a linear relationship, which implies that Eu^{3+} can form single complex with Mo in different concentrations of Morin. The value of $n = 1.977$ can be obtained showing that single complex $EuMo_2$ is formed. Also, the UV-vis absorbance spectrum of 5.0×10^{-5} M Morin and titration of it with different concentrations of Eu^{3+} in a 0.1 M HOAc–NaOAc (pH 6.4) buffer solution is investigated. The UV-vis spectrum of Morin shows an intense absorbance at 388 nm (Band I) and at 263 nm (Band II). Band I is related to ring **B** (cinnamoyl system) and Band II to ring **A** (benzoyl system) (Scheme 1).[31, 32] When 2.0×10^{-4}M Eu^{3+} added to the solution, Band I gradually shifts to 404 nm and shows a lower intense absorbance and band II was unaltered (figures not shown). The results indicated that Morin could form a complex with Eu^{3+}. The results show that the framework of Band I is not changed and Band I has red shifts by ca. 16 nm suggesting that Eu^{3+} have bonded in ring **B**. It can be explained by a bond of Eu^{3+} with the 3–OH group of

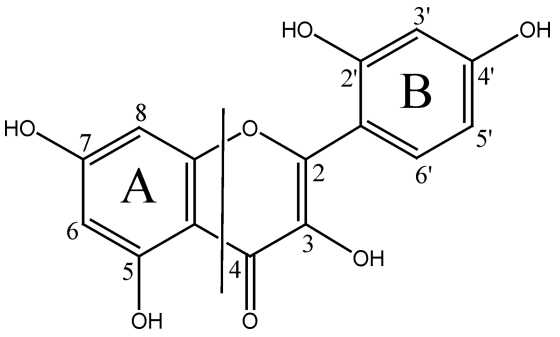

SCHEME 1 Structure of Morin.

Morin to bring electronic redistribution between the Morin molecule and Eu^{3+} resulting in an extended π bond system. Electron transition of Morin changed from n–π^* transition to π–π^* transition and energy of the electron transition decreased. Morin can attract the π bond electron cloud resulting in a polarization that leads to a decreasing difference of π–π^* energy level and absorbance bond red shift.

3.2. Electrochemical Behavior of EuMo2

3.2.1. Electrochemical Behavior of $EuMo_2$

As shown in Figure 3, on the bare GCE, the cyclic voltammogram of $EuMo_2$ demonstrated an irreversible oxidation current peak (E_{pc} =

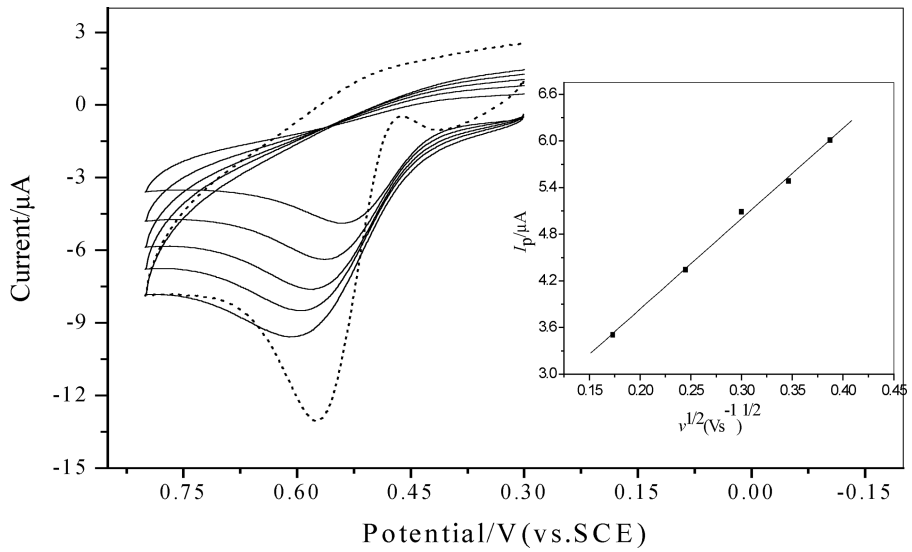

FIGURE 3 Main panel: Cyclic voltammograms of 1.0×10^{-4} M Morin + 2×10^{-4} M Eu^{3+} in Tris–HCl (pH6.4) buffer solution at the GCE at different scan rate. Scan rate: 30, 60, 90, 120, 150 mVs^{-1} (from inside to outside). The dot line represents the elimination current. The inserts show: relationship between I_{pc} and square roots of scan rates, reference scan rate: $60mVs^{-1}$. Rest time: 2 seconds.

0.578 V). Moreover, plots of peak current (I_{pa}) against the square roots of scan rate are linear over the range from 30 mV s^{-1} to 150 mV s^{-1} with a correlation coefficient of 0.9985. It shows that the electrode reaction is controlled by the diffusion of EuMo2. Meanwhile, according to the method of Dračka et al.,[32–34] a voltammogram that eliminates the charging and kinetic currents with conservation of the diffusion current was obtained. As can be seen from the voltammogram of elimination, the elimination current peak is a single peak, suggesting that the electrode processes is controlled by diffusion.[35,36]

3.2.2. Electrochemical Parameters of $EuMo_2$

The relationship between E_{pa} and lnv, over the range of 0.3–0.5 V will be discussed as follows. For an irreversible electrode reaction process, we may use Equation (8):[36]

$$E_{pa} = E^{o'} + \frac{RT}{\alpha nF}\left\{0.780 + 0.5\ln\frac{\alpha nDFv}{RT} - \ln k_s\right\}, \tag{8}$$

where α is the electron transfer coefficient, k_s is the standard rate constant of surface reaction and $E^{o'}$ is the formal potential. According to Equation (8), the curve of E_{pa} versus lnv should be linear (Figure 4a). k_s can be calculated from the intercept, if the values of $E^{o'}$ and D are known. The value of $E^{o'}$ can be obtained from the intercept of E_{pa} versus v plot on the ordinate by extrapolating the line to $v = 0$. The diffusion coefficient D of $EuMo_2$ is determined by chronocoulomeric method. According to the formula given by Anson:[37,38]

$$Q = \frac{2nFAC(Dt)^{1/2}}{\pi^{1/2}} + Q_{dl} \tag{9}$$

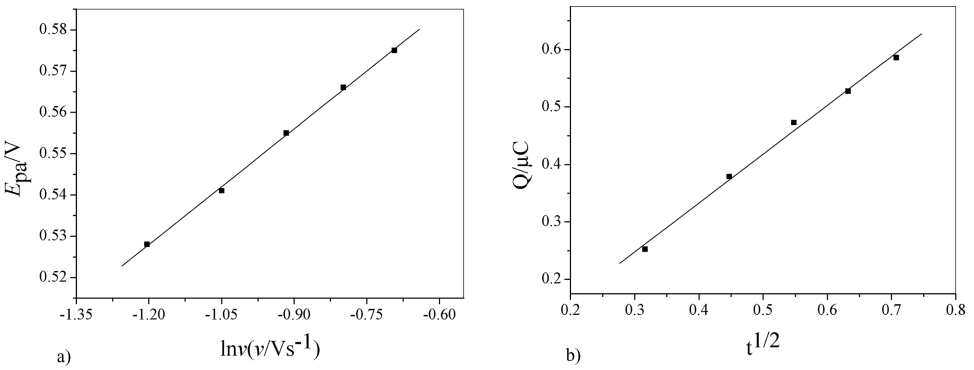

FIGURE 4 Semilogarithmic dependence of the peak potential E_{pa} on the potential scan rate ln$v$ (a) and chronocoulometric dependence of charge on the square roots of time (b) for 2.0×10^{-4} M $EuMo_2$ at the GC electrode.

where Q_{dl} is the double-layer charge (integration of charging current). From the slope of the linear relationship between Q and $t^{1/2}$, D can be determined if C (concentration), A (surface area of the electrode), and n (electron transfer number) are known. From the slope of plot between Q and $t^{1/2}$ (Fig.4b), D was calculated as 2.02936×10^{-6} cm^2 s^{-1}. Thus, the rate constant k_s was calculated as 2.71×10^{-3} cm s^{-1}.

3.3. Interaction of dsDNA with $EuMo_2$

Figure 5 shows the cyclic voltammograms of 5 mM $Fe(CN)_6^{3-/4-}$ +0.1 M KCl supporting electrolyte at a bare GCE (curve a). It can be seen that a pair of redox peaks appear at 0.135 V (E_{pc}) and 0.229 V (E_{pa}), and the peak to peak (ΔE) separation is 99 mV can be obtained at the bare glass carbon electrode. However, at dsDNA modified glass carbon (curve b), the current of $Fe(CN)_6^{3-/4-}$ is dramatically decreased and the ΔE is enhanced sharply by 83 mV. This result indicated that dsDNA is modified on the electrode and demonstrates the existence of coulomb repulsion between the Fe(CN)63-/4- and dsDNA phosphate framework.

3.3.2. Investigation with Electrochemical Methods

Figure 6 is the CV curve for $EuMo_2$ complex at the bare glassy carbon electrode and at the dsDNA-GCE. An oxidation peak of $EuMo_2$ complex appears at 0.650 V at bare GCE (curve a). However, at dsDNA-GCE, the

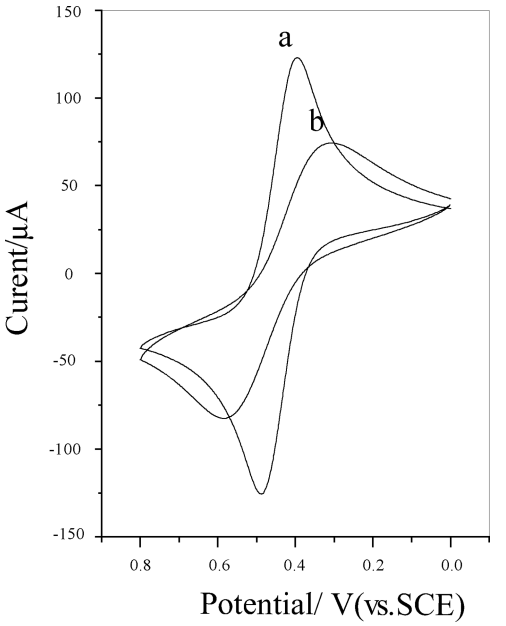

FIGURE 5 Cyclic voltammogram of 5 mM $Fe(CN)_6^{3-/4-}$ containing 0.1 M KCl supporting electrolyte at bare glass carbon electrode (a) and at DNA-modified glass carbon (b); scan rate, 100 mVs^{-1}.

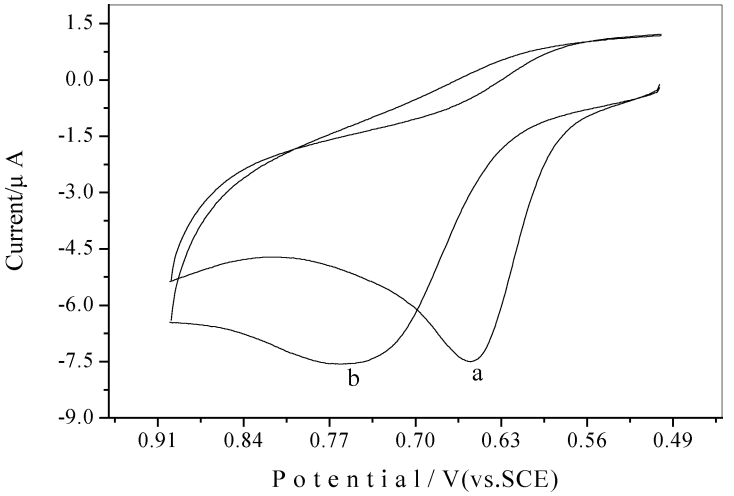

FIGURE 6 Cyclic voltammograms of 2.0×10^{-4} M Mo and 4.0×10^{-4} M Eu^{3+} in 0.1 M Tris–HCl (pH 6.4) buffer containing 50 mM KCl at bare GCE (a) and DNA modified GCE (b); scan rate: 100 mVs^{-1}.

peak have a considerably positive shifts and the peak current is decreased in a 0.1 M HOAc–NaOAc buffer solution (pH 6.4) (curve b). The reason for this might be that 2′,4′-adjacent dihydroxy substituent on the planar aromatic **B**-ring of Morin, the electrochemical active site, can intercalate between the adjacent base pairs of DNA. Peak currents decrease and E_{pa} shifts in a positive direction because the electrochemical active site of the $EuMo_2$ complex intercalates dsDNA.

The relationship between the coulometric charge (Q) for the $EuMo_2$ bound to a dsDNA-GCE and the solution concentration (C) of $EuMo_2$ is presented in Figure 7. It can be seen that the data are well described by the Langmuir model.[38,40] To further quantify the complex binding activities on dsDNA-GCE, we determined the binding constants of $EuMo_2$ with DNA based on the Langmuir model. This classical model assumes that every binding site is equivalent and that the ability of a molecule to bind is independent of the occupation of nearby sites. Non-linearized and linearized forms of the Langmuir isotherm in terms of the redox species concentration, C, the accumulated charge at the electrode surface, Q, and the saturated charge, Q_{sat}, are given by Equation (10), respectively.

$$Q = \frac{Q_{sat} K C}{1 + K C} \tag{10}$$

and its derivative of Equation (11)

$$\frac{C}{Q} = \frac{C}{Q_{sat}} + \frac{1}{K Q_{sat}} \tag{11}$$

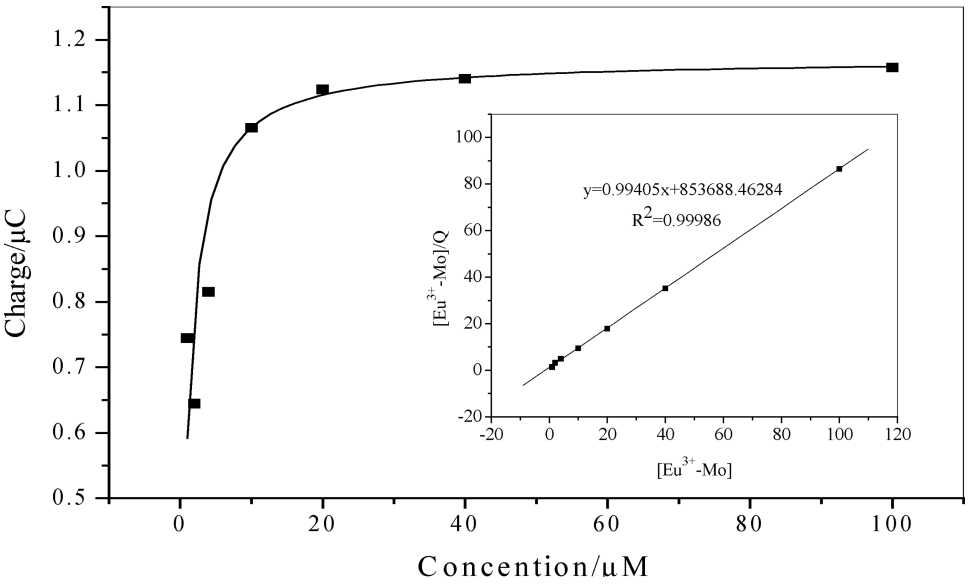

FIGURE 7 Coulometric charge: Q vs $EuMo_2$ concentration dsDNA modified GCE. Insert: Relationship between $[EuMo_2]/Q$ and $[EuMo_2]$ at dsDNA modified GCE. Solid lines are fit to the Langmuir model.

The curve fitting give a saturation charge of $Q_{sat} = 1.14 \times 10^{-6}$ C, corresponding to a surface binding constant of $K = 1.02 \times 10^6$ M^{-1}. In general, the binding affinities of metal complexes with DNA are the order of intercalation ($K > 10^6$ M^{-1})>hydrophobic interaction ($K > 10^5$ M^{-1})>electrostatic interaction ($K > 10^3$ M^{-1}).[11] The K of $EuMo_2$ with DNA is mainly characteristic of intercalation behavior. A saturation coverage value (Γ_s) of 2.51×10^{-10} mol cm^{-2} for $EuMo_2$ at dsDNA-GCE could also be obtained from the fit curve. The oxidation charge (Q) of the dsDNA on the dsDNA modified electrode was 2.08×10^{-6} C, from which a surface coverage value Γ_{dsDNA} of 2.89×10^{-10} mol cm^{-2} (in base pairs) could be determined assuming transfer of 5.45 electrons per base pair.[41] Combining this with the value of Γ_s of 2.51×10^{-10} mol cm^{-2} for $EuMo_2$ at dsDNA-GCE, the ratio of $EuMo_2$ to base pairs of dsDNA on the surface was determined to be 1.16. That is to say, one base pair can bind one molecule of $EuMo_2$.

3.3.3. The Effect of $EuMo_2$ on the Emission Spectra of the DNA-EB System

Further support for the interaction modes of $EuMo_2$ binding to DNA is given through the emission quenching experiment. Here, EB was also employed as a probe. The experiment was carried out in a 3 ml solution of 2.7×10^{-6} M EB, 8×10^{-5} M DNA (at saturating binding levels[42]) titrated with 4×10^{-5} M $EuMo_2$ solution. Figure 8 shows the emission spectra of the DNA-EB system in the presence of $EuMo_2$. The emission intensity of

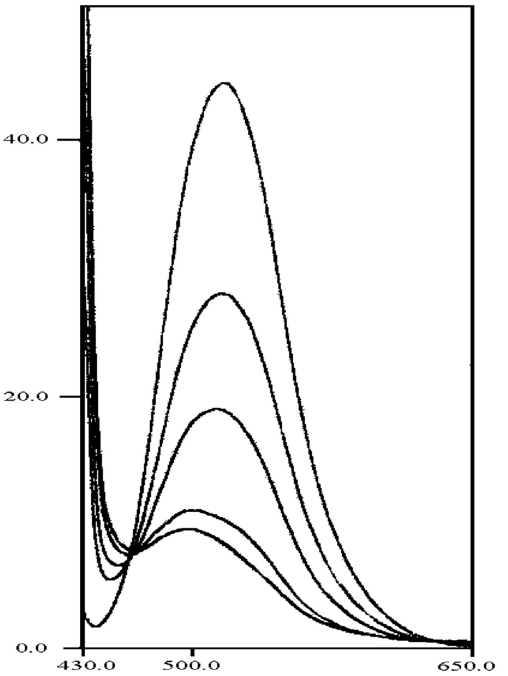

FIGURE 8 Emission spectra (excited at 427 nm): DNA-EB system (2.7×10^{-6} M EB, 8.0×10^{-5} M DNA) in the absence (dotted line) and presence (solid line) of increasing amounts of 1.0×10^{-4} M $EuMo_2$ (20 ml per scan).

the DNA-EB system decreased as the concentration of $EuMo_2$ increased. The changes observed here are often characteristic of intercalation.[43] This phenomenon indicated that $EuMo_2$ replaced EB from the DNA-EB system leading to the emission decrease of the DNA-EB system. The shift was caused by EB changing from a hydrophobic environment into the water solution.

According to the classical Stern-Volmer equation:[44]

$$F_0/F = 1 + k_q[Q],$$

where F_0/F represents the ratio of emission intensity in the absence and presence of quencher, k_q is the quenching constant, $[Q]$ is the concentration of quencher. Static or dynamic quenching process plots of F_0/F versus $[Q]$ appear linear and k_q depends on temperature.[45] The shape of the Stern-Volmer plots can be used to characterize the quenching as being predominantly dynamic or static. The emission quenching of $EuMo_2$ to DNA-EB system at 25°C is shown in Figure 9. Plotting F_0/F versus [$EuMo_2$] appears approximately linear. These changes may suggest that only one kind of quenching process is involved and that $EuMo_2$ binds to DNA mainly by one mode.

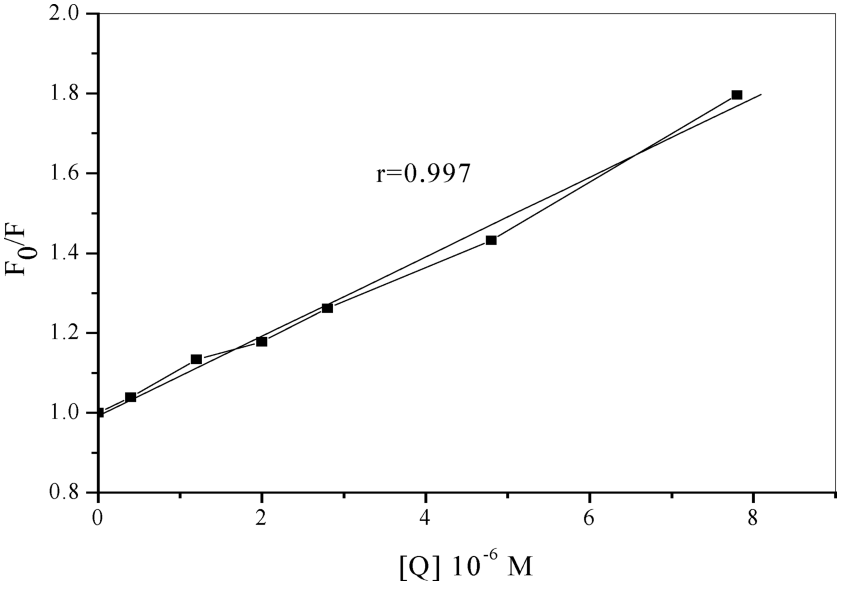

FIGURE 9 Fluoresence quenching of DNA-EB system by [$EuMo_2$].

4. CONCLUSION

In this article, we studied the interaction between Eu^{3+} and Morin, which can form EuMo2 complexes. Also, the electrochemical behavior of $EuMo_2$ and its interaction with calf thymus have been studied. $EuMo_2$ can bind to DNA mainly by intercalation attraction. In addition, the diffusion coefficient ($D = 2.02936 \times 10^{-6}$ cm^2 s^{-1}), rate constant ($k_s = 2.71 \times 10^{-3}$ cm s^{-1}) and the binding constant ($K = 1.02 \times 10^6$ M^{-1}), binding numbers ($n = 1$) of complex per DNA (bp) were obtained. The results provide new insight into rational drug design and would lead us to further understanding of the interaction mechanism between antitumor drug and DNA.

REFERENCES

1. Bailly, C.; Colson, P.; Houssies, C.C. The orientation of norfloxacin bound to double-stranded DNA. *Biochem. Biophys. Res. Commun* **1998**, 243, 844–848.
2. Chourpa, I.; Morjani, H.; Riou, J.F.; Manfaait, M. Intracellular molecular interactions of antitumor drug amsacrine (*m*-AMSA) as revealed by surface-enhanced. *Raman Spectrosc. FEBS Lett.* **1996**, 397, 61–64.
3. Cao, Y.; He, X.W. Studies of interaction between Safranine T and double helix DNA by spectral methods. *Spectrochim. Acta, Part A* **1998**, 54, 883–892.
4. Zhou, J.; Wang, L.F.; Tang, N. Antioxidative and anti-tumour activities of solid quercetin metal(II) complexes. *Trans. Met. Chem.* **2001**, 26, 57–63.
5. Alina, B.; Anacona,; Juan, R. Metal complexes of the flavonoid quercetin: antibacterial properties. *Transition Met. Chem.* **2001**, 26, 20–23.
6. Qu, F.; Li, N.Q.; Jiang, Y.Y. Electrochemical studies of NiTMpyP and interaction with DNA. *Talanta* **1998**, 45, 787–793.

7. Ibrahim, M.S. Voltammetric studies of the interaction of nogalamycin antitumor drug with DNA. *Anal. Chim. Acta* **2001**, 443, 63–72.
8. Zhou, J.; Wang, L.F.; Tang, N. The mechanisms of the binding of quercetin•$2H_2$ O and $LaL_3 \cdot 6H_2O$ to ctDNA. *Indian J. Chem. A* **2001**, 40, 149–154.
9. Zhao, Y.D.; Pang, D.W.; Wang, Z.L.; Cheng, J.K.; Qi, Y.P. DNA-modified electrodes. Part 2. Electrochemical characterization of gold electrodes modified with DNA. *J. Electroanal. Chem* **1997**, 431, 203–209.
10. Liu, S.Q.; Xu, J.J.; Chen, H.Y. ZrO2 gel-derived DNA-modified electrode and the effect of lanthanide on its electron transfer behavior. *Bioelectrochemistry* **2002**, 57, 149–154.
11. Maruyama, K.; Mishima, Y.; Minagawa, K.; Motonaka, J. Electrochemical and DNA-binding properties of dipyridophenazine complexes of osmium(II). *J. Electroanal. Chem.* **2001**, 510, 96–102.
12. Wang, J.; Rivas, G.; Luo, D. DNA-modified electrode for the detection of aromatic amines. *Anal. Chem.* **1996**, 68, 4365–4369.
13. Hashimoto, K.; Ito, K.; Isgimori, Y. Sequence-specific gene detection with a gold electrode modified with DNA Probes and an electrochemically active dye. *Anal. Chem.* **1994**, 66, 3830–3833.
14. Wang, J.; Cai, Rivas.X.G. DNA-Modified Electrode for the Detection of Aromatic Amines. *Anal. Chem.* **1996**, 68, 4365–4369.
15. Cai, H.; Xu, C.; He, P.G.; Y. Fang, Z. Colloid Au-enhanced DNA immobilization for the electrochemical detection of sequence-specific DNA. *J. Electroanal. Chem.* **2001**, 510, 78–85.
16. Jelen, F.; Erdem, A.; Palecek, E. Cyclic voltammetry of echinomycin and its interaction with double-stranded and single-stranded DNA adsorbed at the electrode. *Bioelectrochemistry* **2002**, 55, 165–167.
17. Wang, G.; Xu, J.J.; Chen, H.Y. Interfacing cytochrome *c* to electrodes with a DNA—carbon nanotube composite film. *Electrochem. Commun* **2002**, 4, 506–609.
18. Macias, B.; Villa, M.V.; Fiz, E. Crystal structure of Cu(N-quinolin-8-yl-p-toluenesulfonamidate)2]: study of its interaction with DNA and hydrogen peroxide. *J. Inorg. Biochem.* **2002**, 88, 101–107.
19. Cornard, J.P.; Merlin, J.C. Spectroscopic and structural study of complexes of quercetin with Al(III). *J. Inorg. Biochem.* **2002**, 92, 19–27.
20. Chantal, C.L.M.; France, V.M. Muriel, T.; Helene, S.M.; Jacques, M.; Marc, S.W.; Comparative effects of flavonoids and model inducers on drug-metabolizing enzymes in rat liver. *Toxicology* **1996**, 114, 19–27.
21. Hollman, P.C.H.; Katan, M.B. Dietary flavonoids: Intake, Health effects and bioavailability. *Food Chem. Toxicol.* **1999**, 37, 937–942.
22. Polissero, C.; Lenczowski, M.J.P.; Chinzl, D.; Davail, C.B.; Sumpter, J.P.; Fostier, A. Effects of flavonoids on aromatase activity, an in vitro study. *J. Steroid Biochem. Mol. Biol.* **1996**, 57, 215–223.
23. Ishikawa, Y.; Kitamura, M. Bioflavonoid Quercetin Inhibits Mitosis and Apoptosis of Glomerular Cells *in Vitro* and *in Vivo*. *Biochem. Biophys. Res. Commun.* **2000**, 20, 629–634.
24. Kang, T.B.; Liang, N.C. Studies on the inhibitory effects of quercetin on the growth of HL-60 leukemia cells. *Biochem. Pharmacol.* **1997**, 54, 1013–1018.
25. Yoshiharu, M.; Hitomi, T.; Hirotami, M.; Mikihiko, N.; Takashi, T.; Hisakazu, O.; Yasufumi, S. Effect of bioflavonoids on vincristine transport across blood-brain barrier. *Euro. J. Pharmacol.* **2000**, 3, 193–201.
26. Zhu, Z.; Li, C.; Li, N.Q. Electrochemical studies of quercetin interacting with DNA. *Microchem. J.* **2002**, 71, 57–63.
27. Chen, X.A.; He, Q.C.; Guan, T.; Cheng, Y.E.; Chen, H.F.; Xiong, B.K. Citric acid rare earth complexes on influence of devouring leucocyte of mice. *Chin. J. Rare Earths* **1995**, 1, 70–73.
28. Kang, J.W.; Zhou, L.; Lu, X.Q.; Liu, H.D.; Zhang, M.; Wu, H.X. Electrochemical investigation on interaction between DNA with quercetin and Eu–Qu3 complex. *J. Inorg. Biochem.* **2004**, 98, 79–86.
29. Wang, Z.X.; Liu, D.J.; Dong, S.J. Interactions of Safranin T with nucleic acids. *J. Chem. Chin.* **2001**, 19, 662–669.
30. Zhou, J.; Wang, L.F.; Wang, J.Y.; Tang, N. Synthesis, characterization, antioxidative and antitumor activities of solid quercetin rare earth(III) complexes. *J. Inorg. Biochem.* **2001**, 83, 41–48.
31. Deng, H.; Berkel, G.J.V. Electrospray mass spectrometry and UV/visible spectrophotometry studies of aluminum(III)-flavonoid complexes. *J. Mass Spectrom.* **1998**, 33, 1080–1087.
32. Dračka, O. Theory of current elimination in linear scan voltammetry. *J. Electroanal. Chem.* **1996**, 402, 19–28.
33. Trnková, L.; Dračka, O. Elimination voltammetry. Experimental verification and extension of theoretical results. *J. Electroanal. Chem.* **1996**, 413, 123–129.

34. Trnková, L.; Kizek, R.; Dračka, O. Application of Elimination Voltammetry to Adsorptive Stripping of DNA. *Electroanalysis* **2000**, 12, 905–911.
35. Bard, A.J.; Faulkner, L.R. *Electrochemical Methods, Fundamentals and Applications*. John Wiley: New York, 1980.
36. Kang, J.W.; Li, Z.F.; Lu, X.Q.; Wang, Y.S. Studies on the electrochemical behavior of 3-nitrobenzaldehyde thiosemicarbazone at glass carbon electrode modified with nano-γ-Al2O3. *Elecrochim. Acta* **2004**, 50, 19–26.
37. Anson, F.R. Innovations in the Study of Adsorbed Reactants by Chronocoulometry. *Anal. Chem.* **1966**, 38, 54–57.
38. Anson, F.R. Application of potentiostatic current integration to the study of the adsorption of cobalt(III)-(ethylenedinitrilo(tetraacetate) on mercury electrodes. *Anal. Chem.* **1964**, 36, 932–934.
39. Ozsoz, M.; Erdem, A.; Kara, P.; Kerman, K.; Ozkan, D. Electrochemical biosensor for the detection of interaction between arsenic trioxide and DNA based on guanine signal. *Electroanalysis* **2003**, 15, 613–619.
40. Yu, H.Z.; Luo, C.Y.; Sankar, C.G.; Sen, D. Voltammetric procedure for examining DNA-modified surfaces: Quantitation, cationic binding activity, and electron-transfer kinetics. *Anal. Chem.* **2003**, 75, 3902–3907.
41. Pang, D.W.; Abruna, H.D. Micromethod for the investigation of the interactions between DNA and redox-active molecules. *Anal. Chem.* **1998**, 70, 3162–3169.
42. Barton, J.K.; Goldberg, J.M.; Kumar, C.V.; Turro, N.J. Binding modes and base specificity of tris(phenanthroline)ruthenium(II) enantiomers with nucleic acids: tuning the stereoselectivity. *J. Am. Chem. Soc.* **1986**, 108, 2081–2088.
43. Kumar, C.V.; Barton, J.K.; Turro, M.J. Photophysics of ruthenium complexes bound to double helical DNA. *J. Am. Chem. Soc.* **1985**, 107, 5518–5523.
44. Efink, M.R.; Ghiron, C.A. Fluorescence quenching studies with proteins. *Anal. Biochem.* **1981**, 114, 199–227.
45. Shengdu, L. *Current Protocols for Molecular Biology*. Higher Education Press: Beijing, 1993.